

Ritonavir inhibits intratumoral docetaxel metabolism and enhances docetaxel antitumor activity in an immunocompetent mouse breast cancer model

Jeroen J.M.A. Hendriks^{1,2}, Jurjen S. Lagas¹, Ji-Ying Song³, Hilde Rosing¹, Jan H.M. Schellens^{4,5}, Jos H. Beijnen^{1,5}, Sven Rottenberg² and Alfred H. Schinkel²

¹Department of Pharmacy & Pharmacology, The Netherlands Cancer Institute, Amsterdam, The Netherlands

²Division of Molecular Oncology, The Netherlands Cancer Institute, Amsterdam, The Netherlands

³Department of Experimental Animal Pathology, The Netherlands Cancer Institute, Amsterdam, The Netherlands

⁴Department of Clinical Pharmacology, The Netherlands Cancer Institute, Amsterdam, The Netherlands

⁵Department of Pharmaceutical Sciences, Utrecht University, Utrecht, The Netherlands

Docetaxel (Taxotere[®]) is currently used intravenously as an anticancer agent and is primarily metabolized by Cytochrome P450 3A (CYP3A). The HIV protease inhibitor ritonavir, a strong CYP3A4 inhibitor, decreased first-pass metabolism of orally administered docetaxel. Anticancer effects of ritonavir itself have also been described. We here aimed to test whether ritonavir co-administration could decrease intratumoral metabolism of intravenously administered docetaxel and thus increase the antitumor activity of docetaxel in an orthotopic, immunocompetent mouse model for breast cancer. Spontaneously arising *K14cre;Brca1^{F/F};p53^{F/F}* mouse mammary tumors were orthotopically implanted in syngeneic mice lacking *Cyp3a* (*Cyp3a^{-/-}*) to limit ritonavir effects on systemic docetaxel clearance. Over 3 weeks, docetaxel (20 mg/kg) was administered intravenously once weekly, with or without ritonavir (12.5 mg/kg) administered orally for 5 days per week. Untreated mice were used as control for tumor growth. Ritonavir treatment alone did not significantly affect the median time of survival (14 vs. 10 days). Median time of survival in docetaxel-treated mice was 54 days. Ritonavir co-treatment significantly increased this to 66 days, and substantially reduced relative average tumor size, without altering tumor histology. Concentrations of the major docetaxel metabolite M2 in tumor tissue were reduced by ritonavir co-administration, whereas tumor RNA expression of *Cyp3a* was unaltered. In this breast cancer model, we observed no direct antitumor effect of ritonavir alone, but we found enhanced efficacy of docetaxel treatment when combined with ritonavir. Our data, therefore, suggest that decreased docetaxel metabolism inside the tumor as a result of *Cyp3a* inhibition contributes to increased antitumor activity.

Docetaxel (Taxotere[®]) is currently used as an intravenous anticancer agent for several types of cancer, among which lung, breast, gastric and prostate cancer.¹⁻⁴ The development of an oral formulation of docetaxel is the focus of preclinical and clinical research in our groups. Docetaxel is primarily

metabolized by Cytochrome P450 (CYP) 3A4 and we previously showed that the HIV protease inhibitor and strong CYP3A4 inhibitor ritonavir could decrease first-pass metabolism of docetaxel.^{5,6} As a result, co-administration of the oral formulation of docetaxel with ritonavir results in strongly

Key words: docetaxel, ritonavir, breast cancer, antitumor activity, *Cyp3a* inhibition

Abbreviations: *Bcrp*: gene encoding for breast cancer resistance protein; CYP: Cytochrome P450; *Cyp3a^{-/-}*: *Cyp* knockout mice; EAF: ethanol/acetic acid/formaldehyde/saline fixative at 40:5:10:45% v/v; GEMM: genetically engineered mouse model; *K14cre;Brca1^{F/F}; p53^{F/F}*: mouse model for hereditary breast cancer with spontaneously arising tumors in mammary glands; i.v.: intravenous; LC-MS/MS: liquid chromatography coupled with tandem mass spectrometry; MDR1: P-glycoprotein; *Mdr1a/b*: genes encoding for P-glycoprotein; P-gp: P-glycoprotein; RT-PCR: real-time polymerase chain reaction; SD: standard deviation

Sven Rottenberg's current address is: Institute of Animal Pathology, Vetsuisse Faculty, University of Bern, Switzerland

Additional Supporting Information may be found in the online version of this article.

Conflicts of Interest: The research group of A.H. Schinkel receives revenue from commercial distribution of some of the mouse strains used in this study. J.H.M. Schellens and J.H. Beijnen are inventors on patents on the application of oral taxane formulations and hold stock in the start-up company Modra Pharmaceuticals, a company developing oral taxanes.

Financial support: none

DOI: 10.1002/ijc.29812

History: Received 24 Apr 2015; Accepted 3 Aug 2015; Online 21 Aug 2015

Correspondence to: Jeroen Hendriks, Department of Pharmacy & Pharmacology, The Netherlands Cancer Institute, Amsterdam, The Netherlands, Tel.: 0031 205 125 088, E-mail: jeroen.hendriks@slz.nl

What's new?

The anticancer drug docetaxel is extensively metabolized by the CYP3A enzyme, the activity of which can be blocked by the protease inhibitor ritonavir. Here, in Cyp3A-deficient mice orthotopically implanted with spontaneously arising Cyp3A-expressing mammary tumors, tumor size was found to be significantly reduced by co-administration of docetaxel and ritonavir. Within mammary tumors, Cyp3a inhibition by ritonavir was associated with decreased local docetaxel metabolism, which in turn increased the antitumor activity of docetaxel. Tumor histology was unchanged by the addition of ritonavir, suggesting that the drug has no direct antitumor effects.

increased docetaxel plasma concentrations in mice and human.^{7,8}

Since expression of CYP3A4 has also been reported in tumor tissue of breast, colorectal, and oesophageal cancer and Ewing's sarcoma^{9–13}, intratumoral metabolism of docetaxel could possibly also decrease the response to docetaxel treatment.¹⁴ Thus, co-administration with CYP3A4 inhibitors like ritonavir may also decrease intratumoral CYP3A4-mediated metabolism of docetaxel. A clinical impact of CYP3A4 expression in tumors was further suggested by Murray *et al.*,¹² who found a correlation between strong CYP3A4 expression in tumor tissue and decreased survival of women with breast cancer.

Possible anticancer effects of protease inhibitors themselves, among which ritonavir, have been incidentally described. Ritonavir causes DNA damage and cell death in human endothelial cells.¹⁵ It has also been reported that ritonavir decreases the production of factors that contribute to tumor neovascularisation in Kaposi sarcoma.¹⁶ Based on the inhibitory effect on endothelial cell invasion, ritonavir might inhibit angiogenesis.¹⁷

In vivo, ritonavir treatment decreased tumor growth in an HIV-independent Kaposi sarcoma mouse model.¹⁶ Preclinical antitumor effects of ritonavir were also described for other types of cancer such as mouse lymphoma,¹⁸ human head and neck carcinoma¹⁹ and human breast cancer.²⁰ On the other hand, no antitumor effect of ritonavir was observed for glioblastoma in preclinical and clinical studies.^{21,22}

In earlier studies of a mouse xenograft model of human prostate cancer, ritonavir co-administration increased docetaxel antitumor activity and blocked docetaxel-induced upregulation of CYP3A.²³ However, this study performed in Cyp3a-proficient, immunodeficient mice did not analyze changes in docetaxel plasma levels. At the administered dose of 12.5 mg/kg ritonavir for 5 days a week, inhibition of docetaxel metabolism was likely almost complete. *In vitro*, ritonavir completely blocks docetaxel metabolism at a concentration of ~2.5 μ M.²⁴ This concentration was most likely reached in the *in vivo* situation, as 30 min after single oral administration of 40 mg/kg ritonavir to mice, liver concentrations over 40 nmol/g (~40 μ M) were observed.²⁵ Therefore, the increased antitumor activity might also be caused by the likely highly increased systemic exposure to docetaxel owing to impaired Cyp3a-mediated metabolism. Since Van Waterschoot *et al.*²⁶ showed that plasma levels of intravenously administered docetaxel are fivefold increased when Cyp3a is absent, plasma levels in the doce-

taxel/ritonavir co-treated group might have been increased up to fivefold. It is therefore impossible to judge whether the improved tumor response reported by Ikezoe *et al.*²³ was caused by altered systemic or tumor docetaxel metabolism, or both.

Also for safety reasons, it is pivotal to distinguish between plasma and tumor concentrations of docetaxel after docetaxel/ritonavir co-treatment. Increased plasma concentrations of docetaxel result in increased toxicity,²⁷ whereas increased tumor concentrations result in increased efficacy.²⁸ If tumor concentrations of docetaxel can be increased without increasing docetaxel plasma concentrations, higher efficacy might be observed without increases in toxicity.

In this study, we aimed to investigate whether ritonavir co-administration increases antitumor activity of docetaxel in an immunocompetent, syngeneic, orthotopic mouse model for breast cancer. We used mice lacking Cyp3a as hosts for the transplanted tumors to avoid the confounding effects on tumor response of increased plasma exposure of docetaxel due to general Cyp3a inhibition by ritonavir. This also allowed us to study the localized effect of ritonavir on docetaxel tumor concentrations and tumor growth. Since the transplanted tumors were not Cyp3a deficient, we hypothesized that ritonavir co-administration could not only affect angiogenesis, but could also increase docetaxel levels in tumor tissue by inhibiting tumor Cyp3a. It has further been reported that docetaxel treatment can induce expression of Cyp3a in tumor tissue in *in vitro* experiments.²⁹ Since it is possible that ritonavir can reduce this induction of Cyp3a back to normal levels,²³ co-administration of ritonavir might also result in relatively decreased docetaxel metabolism by blocking the enhancement of Cyp3a expression. Such possible expression changes were therefore also assessed in this study.

Material and Methods**Drugs and chemicals**

Docetaxel and ritonavir were purchased from Sequoia Research Products (Oxford, UK). Drug-free lithium-heparinized human plasma was obtained from Bioreclamation LLC (New York, NY). All other chemicals were of analytical grade and obtained from commercial sources.

Animals

All mouse experiments were approved by the Animal Experiments Review Board of The Netherlands Cancer Institute

(Amsterdam), complying with Dutch legislation and in accordance with European Directive 86/609/EEC. Mice were kept in a temperature-controlled environment with a 12-hr light/12-hr dark cycle and received a standard diet (AM-II, Hope Farms, Woerden, The Netherlands) and acidified water *ad libitum*. Crushed and moistened food was made available for additional support of mice during treatment. Since we implanted a mouse breast tumor, female recipient mice were selected. In this study, Cyp3a knockout mice (*Cyp3a*^{-/-}) in a >99% FVB genetic background³⁰ were used as host to eliminate differences in systemic docetaxel metabolism between single docetaxel treatment and co-administration of docetaxel and ritonavir. In experiments to test for the maximum tolerable dose, mice of 8–14 weeks of age were used. For tumor implantations, mice of 7–11 weeks of age were used.

Drug solutions

Prior to the experiments, stock solutions containing 18, 24, 30, 36 or 42 mg/mL docetaxel or 7.5 mg/mL ritonavir in ethanol:polysorbate 80 (1:1, v/v) were made and stored at -20°C. On the day of the experiments docetaxel stock solutions were diluted sixfold with saline to obtain solutions for intravenous (i.v.) administration. Solutions containing docetaxel were injected in a volume of 5 µL per g of bodyweight into the tail vein of the mice, in order to achieve a dosage of 15, 20, 25, 30 or 35 mg/kg docetaxel. Ritonavir stock solutions were diluted sixfold with water to obtain solutions for oral administration. Ritonavir was orally administered in a volume of 10 µL per g of bodyweight to the mice, in order to achieve a dosage of 12.5 mg/kg ritonavir. Oral administration was performed by gavage into the stomach using a blunted needle.

Maximum tolerable dose

Prior to tumor treatment, the maximum tolerable dose of docetaxel and ritonavir for *Cyp3a*^{-/-} mice was determined. The maximum tolerable dose was defined as the maximum dose at which mice maintained at least 80% of their initial bodyweight and at which mice did not show signs of little to moderate discomfort (*e.g.*, inactivity, general weakness/illness or neglected coat). Mice were treated with 15, 20, 25, 30 or 35 mg/kg intravenously administered docetaxel or 12.5 mg/kg orally administered ritonavir. Docetaxel was administered once a week, while ritonavir was administered for 5 subsequent days per week. Tolerability of the doses was determined during treatment with docetaxel and/or ritonavir for 3 subsequent weeks.

Tumor implantation

Spontaneously growing tumors from the *K14cre;Brca1*^{F/F};*p53*^{F/F} mouse model³¹ for hereditary breast cancer were expanded *in vivo* without losing their morphologic and biochemical properties.³² A tumor with basal expression of *Cyp3a*, *Mdr1a/b* and *Bcrp* (Breast Cancer Resistance protein) was selected to compare response after docetaxel treatment with and without rito-

navir, and small tumor pieces (1–2 mm) were grafted orthotopically in the mammary fat pad of syngeneic female *Cyp3a*^{-/-} mice as described before.³² In screening experiments, the selected tumor showed a decreased tumor volume after treatment with docetaxel and was therefore considered as docetaxel-sensitive. After implantation, tumor size was measured *in situ* in the living animal by caliper (volume = 0.5 × length × width²).^{33,34} One observer measured all tumors to reduce variation in tumor measurement.³³

Tumor treatment and sample collection

Tumor treatment was started (Day 1) when tumors reached a volume of ~200 mm³. Mice were divided randomly over four groups. Group I was not treated and used as control for tumor growth. Group II was treated with 12.5 mg/kg oral ritonavir, Group III was treated with 20 mg/kg intravenous (i.v.) docetaxel, and Group IV was treated with both 20 mg/kg i.v. docetaxel and 12.5 mg/kg oral ritonavir (Supporting Information Fig. 1). Docetaxel was administered once a week, while ritonavir was administered for 5 subsequent days per week. Mice were treated for 3 subsequent weeks or until tumors reached a volume of ~1,500 mm³. After three weeks, treatment was stopped and mice were monitored until a tumor volume of ~1,500 mm³ was reached. Tumor volumes were measured daily in all groups. At a tumor volume of ~1,500 mm³, mice were sacrificed and blood was taken by cardiac puncture and tumors collected. Blood samples were centrifuged at ambient temperature at 8,000 g for 5 min and subsequently plasma was collected. After tumor isolation, the tumor was cut over its length axis. One half was used for histological analysis and the other half was used for analysis of drug concentrations and RNA expression. Additional mice were used for tumor and plasma sampling on Day 2 and 9. In Groups III and IV, samples were also collected on Day 16. All samples were taken approximately 24 hrs after drug administration on the day before.

Histological analysis

Tumor samples for histological analysis were fixed in EAF fixative (ethanol/acetic acid/formaldehyde/saline at 40:5:10:45 v/v) and embedded in paraffin. Sections were cut at 2 µm from the paraffin blocks, stained with hematoxylin and eosin (HE), and analyzed according to standard procedures. The sections were reviewed with a Zeiss Axioskop2 Plus microscope (Carl Zeiss Microscopy, Jena, Germany) equipped with Plan-Apochroma and Plan-Neofluar objectives. Images were captured with a Zeiss AxioCam HRc digital camera and processed with AxioVision 4 software (both from Carl Zeiss Vision, Munich, Germany).

RNA expression levels

After isolation, tumor samples were stored in RNAlater[®] (Qiagen, Venlo, The Netherlands) until RNA was extracted using the RNeasy mini kit (Qiagen) according to the manufacturer's protocol for the purification of total RNA from

animal tissues. Subsequently, cDNA was generated as described previously.³⁵

Real-time (RT)-PCR was performed on an Applied Biosystems 7,500 real-time cycler system according to the manufacturer's protocol. Specific primers (Qiagen) for the individual mouse genes *Cyp3a11*, *Cyp3a13*, *Cyp3a16*, *Mdr1a*, *Mdr1b* and *Bcrp* were used, and amplification and comparative Ct analysis of the results were performed as described previously.^{35,36} Quantification of the target cDNAs in all samples was normalized to GAPDH cDNA ($Ct_{\text{target}} - Ct_{\text{GAPDH}} = \Delta Ct$). Statistics were performed on ΔCt values.³⁷

Drug concentrations

Previously developed liquid chromatography assays coupled with tandem mass spectrometry detection (LC-MS/MS) were used to quantify docetaxel, ritonavir, and docetaxel metabolites M1/M3, M2 and M4 in plasma and tumor homogenates.^{38,39} Tumor samples were homogenized in 4% of bovine serum albumin in phosphate-buffered saline pH 7.4 (w/v). For quantification of docetaxel, homogenized tumor samples were sixfold diluted with blank human plasma as the concentrations in the undiluted samples were outside the calibration range. Ritonavir and metabolites of docetaxel were quantified in undiluted homogenized tumor samples. In plasma, all drugs were quantified in undiluted samples. Samples were processed as described previously.⁴⁰ Calibration standards in human plasma were used for quantification. Concentrations in homogenized tumor samples were back-calculated to concentrations in tumor tissue. Limits of quantification for docetaxel and its metabolites in plasma and tumor tissue were 0.5 ng/mL and 0.5 ng/g, respectively, and 2 ng/mL and 2 ng/g for ritonavir.

Statistical analysis

The Mann-Whitney *U* test was used when differences in drug levels between two groups were compared. Differences were considered statistically significant when $p < 0.05$. For RNA expression levels, one-way ANOVA with Dunnett's correction was used to accommodate for multiple testing and to compare expression levels to the control group. Differences were considered statistically significant when $p < 0.05$. All data are presented as mean \pm SD. Survival curves were compared using a Log-rank (Mantel-Cox) test. To correct for multiple comparisons, differences between survival curves were considered only statistically significant when $p < 0.00833$. To compare the period to development of a critical tumor volume (1,500 mm³), one-way ANOVA was used and the Bonferroni *post-hoc* correction was used to accommodate for multiple testing. Differences were considered statistically significant when $p < 0.05$.

Results

Maximum tolerable dose of docetaxel and ritonavir

Tolerability of i.v. docetaxel in female *Cyp3a*^{-/-} mice was first assessed. At all tested doses, no signs of little to moderate discomfort were observed other than a decrease in bodyweight. Weekly administrations of doses up to 25 mg/kg i.v. docetaxel

were well tolerated for 3 weeks ($n = 3$ per dose level; data not shown). Administration of 30 or 35 mg/kg i.v. docetaxel resulted in a drop in bodyweight to near 80% of the initial bodyweight for all mice after the third administration of docetaxel ($n = 2$ per dose level). As a result, 25 mg/kg was considered to be the maximum tolerable dose of docetaxel.

Oral administration of 12.5 mg/kg ritonavir (daily, 5 times per week) was also tolerated for 3 weeks ($n = 3$). However, the combination of 25 mg/kg i.v. docetaxel and 12.5 mg/kg ritonavir resulted in an unacceptable decrease in bodyweight (to below 80% of the initial bodyweight) during the third week of treatment ($n = 4$), despite additional support of the mice with crushed and moistened food during treatment. A dose of 15 ($n = 4$) or 20 mg/kg ($n = 5$) i.v. docetaxel co-administered with 12.5 mg/kg oral ritonavir was tolerated when using additional support with crushed and moistened food during treatment. Therefore, 20 mg/kg i.v. docetaxel and 12.5 mg/kg oral ritonavir was selected as the maximum tolerable dose combination of docetaxel and ritonavir and used for tumor treatment (Supporting Information Fig. 1). The selected weekly administration of docetaxel was based on commonly used administration schedules in the clinical setting⁴¹ and ritonavir administration was based on the design of Ikezoe *et al.*²³ to allow optimal comparison of the results.

Effects of drug treatment on tumor growth

When the orthotopically transplanted tumors reached a volume of ~ 200 mm³, the drug treatments were started (Supporting Information Fig. 1). Treatment was given for 3 subsequent weeks. Since tumors of mice receiving only ritonavir reached a volume of $\sim 1,500$ mm³ within 3 weeks, these mice were sacrificed before the end of the initially planned period of treatment. The median time to reach a tumor volume of $\sim 1,500$ mm³ was 10 days in the control group and 14 days in the ritonavir-treated group (Fig. 1). Mean times to reach 1,500 mm³ were 10.8 (SD: 2.2) days and 12.4 (SD: 3.1) days, respectively (Supporting Information Fig. 2). Although the tumors in the ritonavir-treated group tended to grow slightly more slowly, there was no statistically significant difference between the survival curves of the ritonavir-treated group and the untreated group.

As expected, docetaxel treatment alone resulted in a reduction of tumor volume. After three weeks of treatment the tumor volume was reduced to $\sim 70\%$ of the tumor volume at the start of the treatment (Fig. 2). However, after co-treatment with docetaxel and ritonavir the tumor volume was further reduced to $\sim 30\%$ of the initial tumor volume ($p < 0.01$). In line with this stronger effect of co-treatment, the median time to reach a tumor volume of $\sim 1,500$ mm³ was 54 days (mean \pm SD: 53.6 \pm 1.5) in the docetaxel group and 66 days (mean \pm SD: 65.6 \pm 8.6) in the docetaxel and ritonavir group (Fig. 1; Supporting Information Fig. 2). Interestingly, a statistically significant difference ($p = 0.0025$) was observed between the survival curves of the docetaxel-treated group and the docetaxel and ritonavir co-treated group (Fig. 1). Thus, oral co-administration of ritonavir increased the

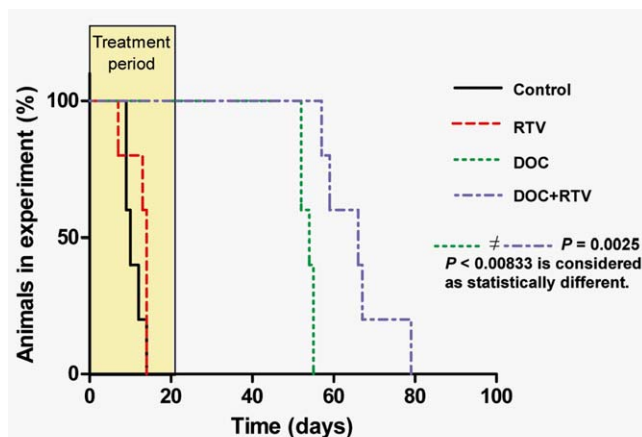


Figure 1. Effect of docetaxel/ritonavir co-administration on survival of *Cyp3a*^{-/-} mice ($n = 5$ per group) with orthotopically implanted syngeneic mouse mammary tumors. Mice were treated for 3 weeks with 20 mg/kg i.v. docetaxel and/or 12.5 mg/kg oral ritonavir. Docetaxel was administered once a week, while ritonavir was administered for 5 subsequent days per week. Untreated mice were used as a control group. Treatment was started at a tumor volume of 200 mm³ and mice were sacrificed when a tumor volume of ~1,500 mm³ was reached. Note that differences between survival curves were considered statistically significant when $p < 0.00833$, in view of the multiple (4) groups compared. [Color figure can be viewed in the online issue, which is available at wileyonlinelibrary.com.]

activity of docetaxel treatment in our model, both in terms of absolute reduction in tumor size and median time to reach a critical tumor size, a surrogate measure for survival.

Histological analysis

Tumor tissue derived from the control group on Day 2 was considered representative for initial tumor tissue. Histological analysis of these samples showed a solid and moderately differentiated adenocarcinoma with thin fibro-vascular stroma and no signs of inflammation (Fig. 3). The tumor cells were round and moderate in size with very poor cell boundaries. Mitotic cells were abundantly present and apoptotic cells were readily seen. Necrosis was locally observed in the tumor tissue. On Day 9, necrosis in tumor tissue of the control group was more extensive and the tumor stroma showed an increased amount of collagen. At a tumor volume of ~1,500 mm³, necrosis of tumor tissue of the control group was even more readily observed than in tumor tissue collected on Day 9. Tumor tissue (including stromal elements such as microvessel density) collected from ritonavir-treated mice was similar to tumor tissue from the control group for Days 2 and 9, and at a tumor volume of ~1,500 mm³. Ritonavir treatment alone therefore did not seem to affect histology of the tumors.

On Day 2, tumor tissue in docetaxel-treated mice showed more apoptosis than tumor tissue in untreated mice. On Day 9, tumor cells of docetaxel-treated mice showed a significant deal of pleomorphism (variability in the size and shape of cells) and

tumor stroma was expanded with fibrotic changes. In these samples, mitotic cells were readily seen, although not as frequently as in untreated tumor tissue. Apoptotic cells were abundantly present and no necrosis was observed in tumor tissue of docetaxel-treated mice on Day 9. On Day 16, the number of mitotic cells was further reduced and atrophic cells were observed. Tumor tissue of ritonavir and docetaxel co-treated mice was very similar to tumor tissue of docetaxel-treated mice. There was no obvious difference in the histopathology of all the tumors, treated or untreated, once they reached a size of ~1,500 mm³ (*i.e.*, when fully grown out, and at least 4 weeks after termination of docetaxel treatment if applied).

RNA expression levels

The observed difference in tumor growth between the docetaxel-treated group and the docetaxel and ritonavir co-treated group might be related to an altered expression profile of docetaxel-metabolizing or -transporting enzymes (*e.g.*, *Cyp3a* or *P-gp*) in the tumors between the groups. We therefore measured RNA expression levels in all tumor tissue samples derived on Days 2, 9 and 16. Although protein activity and RNA expression do not always correlate, we had only very limited tissue available, and thus mRNA expression was measured instead of protein activity. Tissue samples derived from the control group on Day 2 were considered to represent initial expression levels in tumor tissue. Of the various *Cyp3a* genes we found that *Cyp3a11* and *Cyp3a16* were expressed in the tumors. Expression levels of all genes tested were unchanged over time in the control group (Fig. 4). Single treatment with orally administered ritonavir or intravenously administered docetaxel did not change expression levels of *Cyp3a11*, *Cyp3a16* or *Bcrp*. However, repeated single administration of docetaxel resulted in increased expression levels of *Mdr1a* and *1b* on Days 9 and 16 (Fig. 4, panel C and D). This increase during the drug administration period was transient, since expression of *Mdr1a* and *1b* in tumors at a volume of ~1,500 mm³ returned to initial expression levels. After administration of docetaxel with or without ritonavir, expression levels of *Cyp3a11*, *Cyp3a16* or *Bcrp* were not significantly different. Expression levels of *Mdr1a* and *1b* on Day 2 were significantly higher after co-administration of docetaxel and ritonavir, but again similar between the docetaxel and docetaxel plus ritonavir groups on Days 9 and 16, and similar in all tumors at a volume of ~1,500 mm³.

Since expression levels of the tested genes on Days 9 and 16 were not different between docetaxel treatment with and without ritonavir, these results suggest that the increased activity of docetaxel when co-administered with ritonavir cannot be explained by a difference in expression levels of *Cyp3a*, *Mdr1a/1b* or *Bcrp* as a result of ritonavir co-administration.

Drug concentrations in plasma and tumors

On Days 2, 9 and 16, plasma concentrations of ritonavir were below the limit of detection. These samples were taken

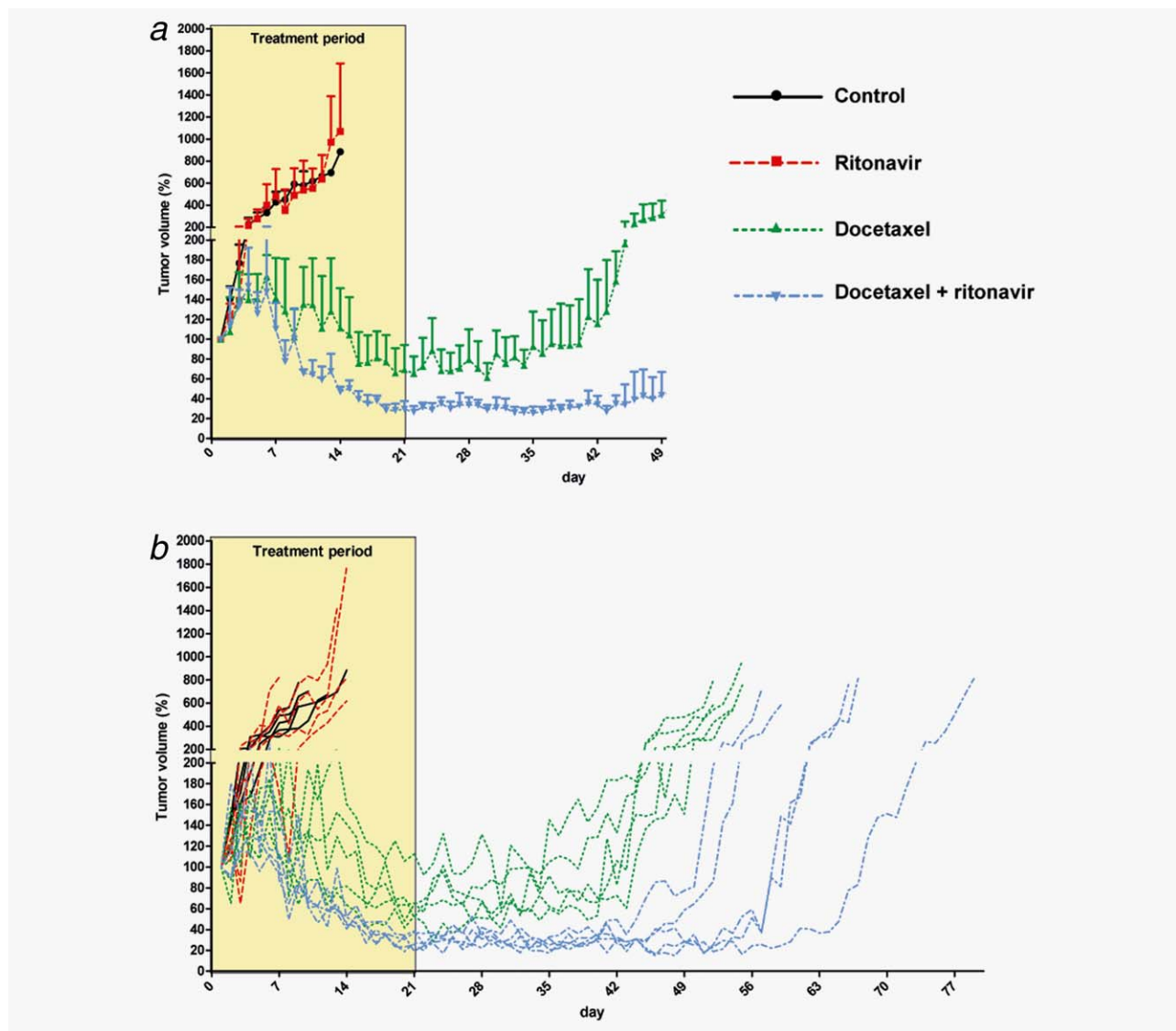


Figure 2. Tumor volumes after docetaxel/ritonavir co-administration to *Cyp3a*^{-/-} mice ($n = 5$ per group) with orthotopically implanted syngeneic mouse mammary tumors. Tumor volumes are presented as percentage of the tumor volume at start of treatment. Mice were treated for 3 weeks and monitored as described in the legend to Figure 1 and in Supporting Information Figure 1. Panel A shows the mean tumor volumes with standard deviations per treatment group over the first 7 weeks. Beyond this period, differential loss of individual mice between groups would result in biased means; these were, therefore, not plotted. Panel B shows the curves of individual mice over the full monitoring period. Curves of different colors represent different treatment groups. [Color figure can be viewed in the online issue, which is available at wileyonlinelibrary.com.]

approximately 24 hrs after oral administration of 12.5 mg/kg ritonavir on the day before. Docetaxel metabolites could also not be detected in plasma samples taken on Days 2, 9 and 16 (approximately 24 hrs after i.v. administration of 20 mg/kg docetaxel). In contrast, docetaxel plasma concentrations were readily detectable throughout, and not significantly different after administration of i.v. docetaxel with or without oral ritonavir ($p > 0.05$, Fig. 5, panel A).

In tumor tissue on Day 2, 24 hr after the first drug administration, both docetaxel and ritonavir concentrations were comparable between single and co-administration of the drugs ($p > 0.05$; Fig. 5, panel B and D). However, on

Day 9, concentrations of docetaxel and ritonavir in tumor tissue were significantly higher when docetaxel was co-administered with ritonavir than after single drug administration ($p < 0.001$). On Day 16, although not statistically significant ($p = 0.15$), tumor concentrations of docetaxel also tended to be increased in the co-treated group. Interestingly, tumor concentrations of the major docetaxel metabolite M2 after docetaxel and ritonavir co-administration were significantly lower than after single docetaxel administration at all tested time points ($p < 0.05$ to $p < 0.01$; Fig. 5, panel C), suggesting substantially decreased metabolism of docetaxel.

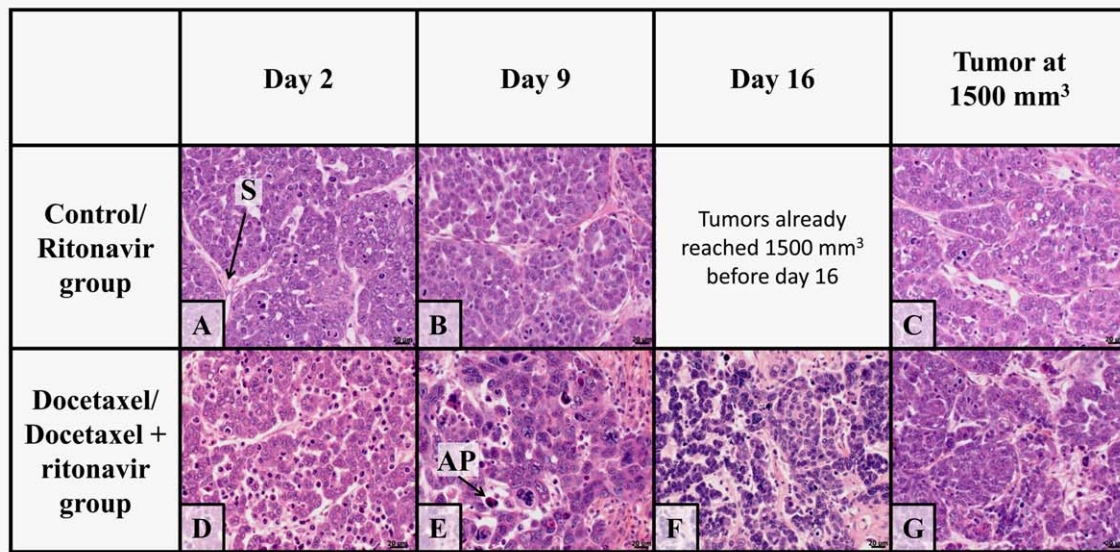


Figure 3. Photomicrographs of representative HE sections of tumor tissue after docetaxel/ritonavir co-administration to *Cyp3a*^{-/-} mice ($n = 5$ per group) with orthotopically implanted syngeneic mouse mammary tumors. Tumor tissues of untreated mice and mice treated with 12.5 mg/kg ritonavir for 5 subsequent days a week were indistinguishable and representative images of the control group are therefore shown in the upper panels. Tumor tissue of mice treated with 20 mg/kg docetaxel once a week also looked very similar with or without co-administration of ritonavir and representative images of the docetaxel-treated group are shown in the lower panels. Mice were sacrificed for pathological examination on Days 2 and 9, and at a tumor volume of $\sim 1,500 \text{ mm}^3$. Docetaxel-treated mice were also sacrificed at Day 16. Tumor tissue derived from the control group at Day 2 was considered as representative for initial tumor tissue (Panel A). Over time, necrosis in tumor tissue became more extensive and the tumor stroma showed an increasing amount of collagen (Panels B and C). On Day 2, tumor tissue in docetaxel-treated mice showed more apoptosis than tumor tissue in untreated mice (Panel D). During docetaxel treatment, tumor cells showed a significant deal of pleomorphism (variability in the size and shape of cells) and the tumor stroma was expanded (Panels E and F). Mitotic cells were readily seen, while apoptotic cells were abundantly present (Panel F). Tumor tissues of tumors of $\sim 1,500 \text{ mm}^3$, when fully grown out, and thus either untreated or at least 4 weeks after the last docetaxel treatment, were not morphologically different between untreated mice and mice treated with docetaxel (Panel G). Arrows mark tumor stroma (S), and apoptosis (AP). (Original magnification 40 \times). [Color figure can be viewed in the online issue, which is available at wileyonlinelibrary.com.]

Discussion

Our data in immunocompetent *Cyp3a*^{-/-} mice with an orthotopically transplanted mouse mammary tumor model revealed a pronounced additional inhibiting effect on tumor growth when oral ritonavir was co-administered with i.v. docetaxel, and an accordingly improved survival time (Figs. 1 and 2). No effect of ritonavir administration alone was observed and histological analysis of tumors showed no qualitative difference between docetaxel treatment with or without ritonavir. Therefore, it is likely that in our experiments the antitumor activity of docetaxel was enhanced by the co-administered ritonavir, instead of reflecting a direct antitumor effect of ritonavir itself.

Previously, antitumor effects of ritonavir treatment have been assessed in multiple mouse models.^{18–20,23} However, most of these mouse models used subcutaneous human xenografts in immunocompromised mice and the predictive value of such models for the clinical setting is often questioned.^{42,43} Genetically engineered mouse models (GEMMs) developing certain well-defined tumors, such as the *BRCA1*- and *p53*-deficient mouse model used here, might be better to predict clinical activity of anticancer drugs, since GEMM-derived tumors evolve in immune-proficient physiological conditions and use

representative tumor-stromal interactions.^{43,44} Mammary tumors in this model have molecular signatures resembling those of human *BRCA1*-mutated breast cancers, and their characteristics are maintained upon transplantation, although they do not metastasize appreciably.³¹ All transplanted tumors grow in the same immunological environment, with the same very limited genetic differences between the tumors and the host. Moreover, spontaneous tumors of this GEMM showed a similar response to docetaxel when different parts of the same tumor were orthotopically transplanted into syngeneic wild-type mice.⁴⁵ Therefore, we used these spontaneous *K14cre;Brca1*^{F/F}; *p53*^{F/F} mouse mammary tumors orthotopically implanted in the mammary fat pad of a syngeneic *Cyp3a*^{-/-} strain, thus avoiding a strong increase in docetaxel plasma concentrations due to inhibition of systemic *Cyp3a* metabolism by ritonavir.

Our results show decreased tumor growth and improved survival after docetaxel and ritonavir co-treatment with comparable plasma exposure as observed after single docetaxel treatment. Unlike Ikezoe *et al.*,²³ who found improved response of prostate cancer xenografts to docetaxel treatment combined with ritonavir, but did not consider altered systemic levels of docetaxel, we can conclude that a main factor in the improved response of

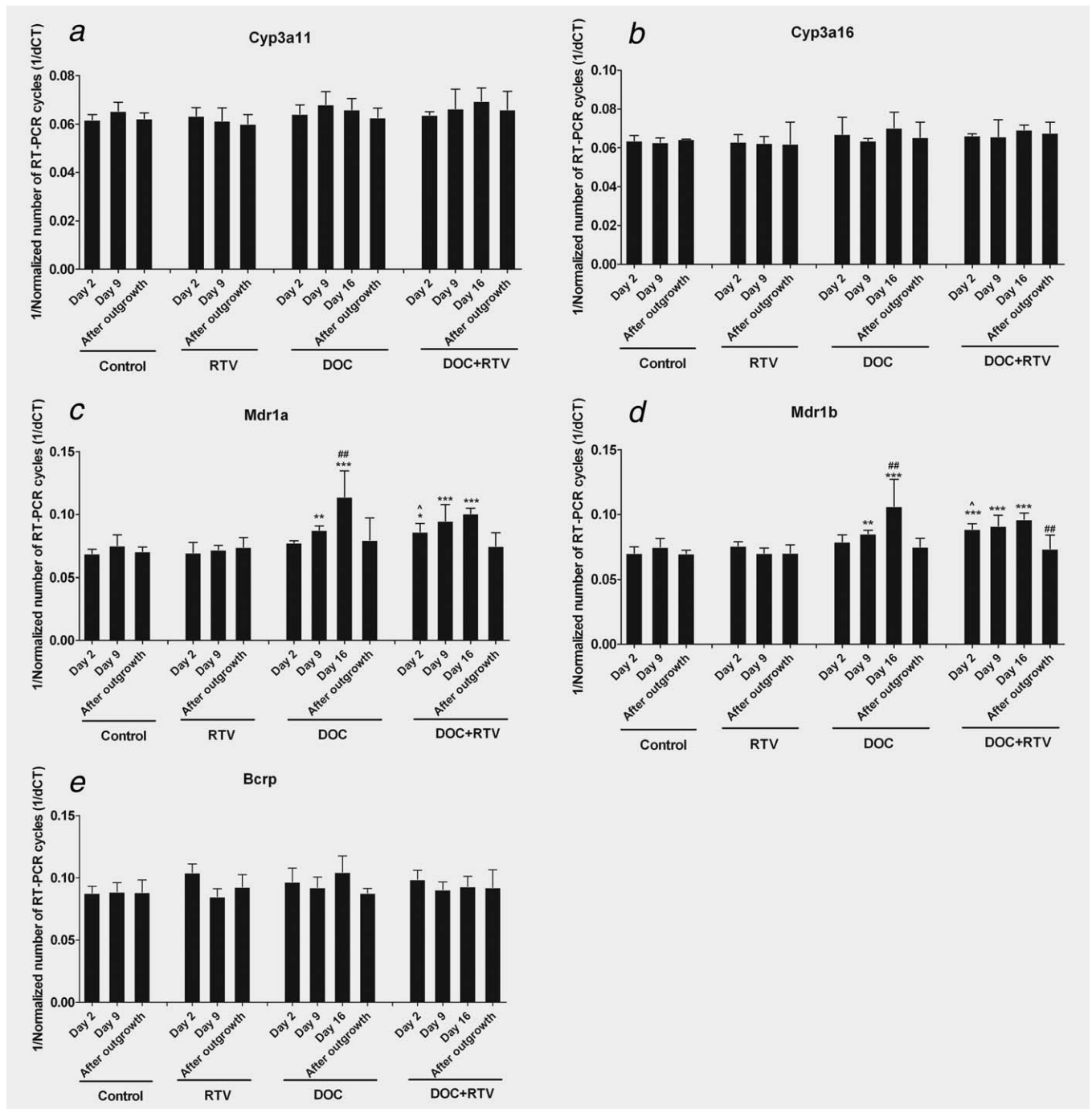


Figure 4. RNA expression levels in tumor tissue ($n = 5$ per group). Panels reflect expression of *Cyp3a11* (panel A), *Cyp3a16* (panel B), *Mdr1a* (panel C), *Mdr1b* (panel D) and *Bcrp* (panel E). Expression of *Cyp3a13* was too low to detect. *Cyp3a*^{-/-} mice were implanted with syngeneic mouse mammary tumors and treated for 3 weeks and monitored as described in the legend to Figure 1 and in Supporting Information figure 1. Untreated mice were used as a control group. Samples were collected on Day 2, Day 9 and after outgrowth (tumor volume $\sim 1,500$ mm³). Samples were also collected on Day 16 for the docetaxel and docetaxel + ritonavir treated group. Data reflect 1 divided by the number of RT-PCR cycles. Data are presented as mean \pm S.D. Cycles are normalized for GAPDH expression. Data are not statistically different from samples taken on Day 2 in the control group, unless otherwise specified (* $p < 0.05$, ** $p < 0.01$ and *** $p < 0.001$). Other symbols reflect a statistical difference between Day 2 and another day in that group (## $p < 0.01$) or a difference between docetaxel treatment with or without ritonavir ($p < 0.05$). Abbreviations: DOC: docetaxel; RTV: ritonavir.

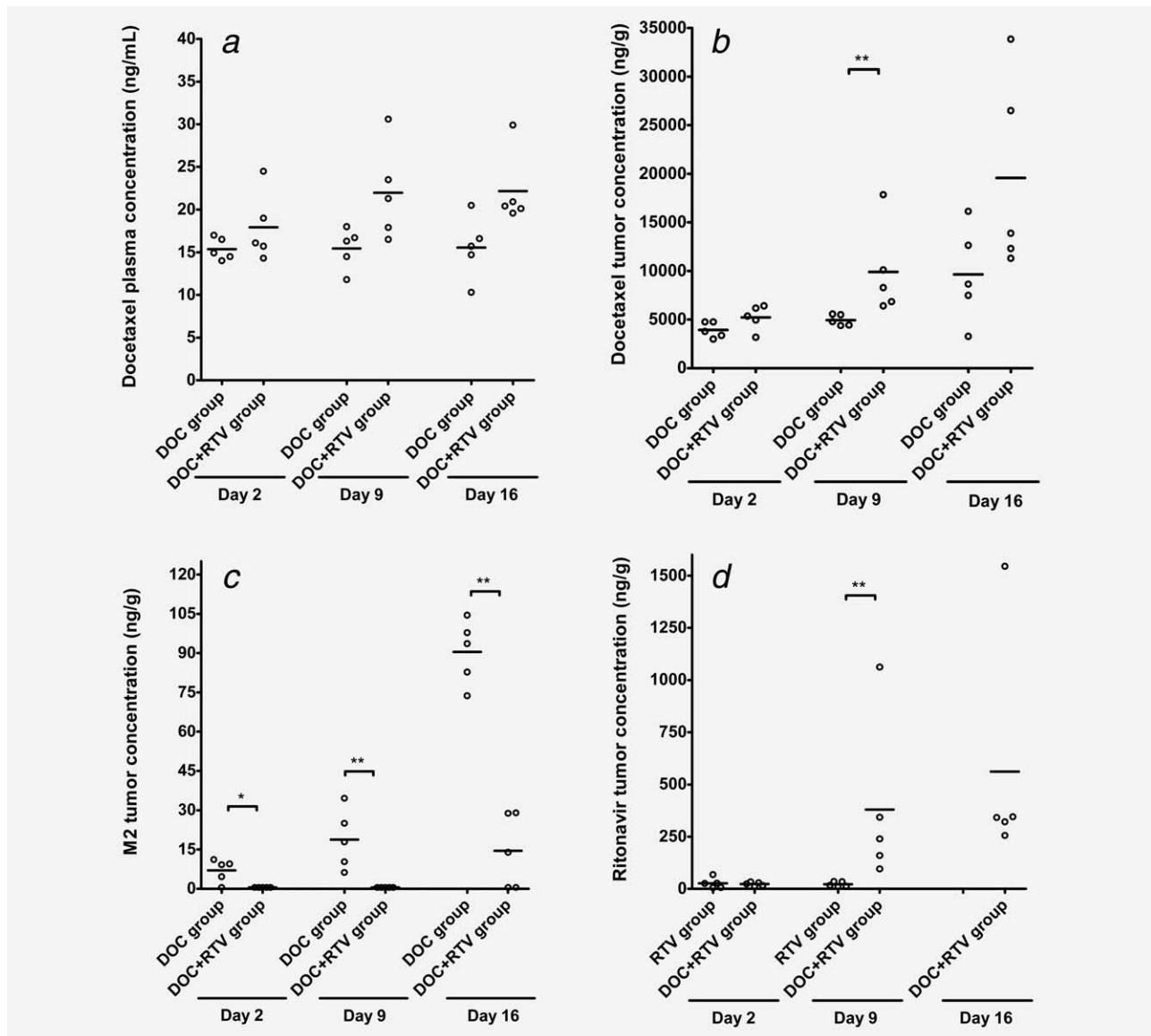


Figure 5. Drug concentrations in plasma and tumor tissue ($n = 5$ per group) on Days 2, 9 and 16. Samples were taken approximately 24 hr after the last administration of ritonavir and docetaxel. Panels reflect plasma (panel A), and tumor (panel B) concentrations of docetaxel, tumor concentrations of docetaxel metabolite M2 (panel C), and tumor concentrations of ritonavir (panel D). Ritonavir and metabolite M2 were not detected in plasma (limit of detection was 2 ng/mL and 0.5 ng/mL, respectively). *Cyp3a*^{-/-} mice were implanted with syngeneic mouse mammary tumors and treated for 3 weeks and monitored as described in the legend to Figure 1 and in Supporting Information Figure 1. Untreated mice were used as a control group. Samples were collected on Days 2 and 9. Samples were also collected on Day 16 for the surviving docetaxel and docetaxel + ritonavir treated groups. Data are presented as individual data points and lines represent the mean. Statistical significance was tested using the Mann-Whitney *U* test. The limit of detection (0.5 ng/g) was used for statistical calculations when tumor concentrations of M2 were below the limit of detection. Differences between single drug treatment and co-treatment of docetaxel and ritonavir are not statistically different, unless otherwise specified (** $p < 0.01$). Abbreviations: DOC: docetaxel; NS: not significant; RTV: ritonavir.

breast tumors to docetaxel and ritonavir co-treatment is likely reduced tumor docetaxel metabolism. This finding is important since, if this drug combination results in increased efficacy independent from docetaxel plasma concentrations, a judicious clinical application may increase docetaxel antitumor efficacy without increasing systemic toxicity.

We aimed to better understand the additional inhibiting effect on tumor growth when oral ritonavir was co-

administered with i.v. docetaxel and studied drug concentrations in plasma and tumor tissue as well as mRNA expression in tumor tissue. After i.v. administration of docetaxel in *Cyp3a*^{-/-} mice, plasma concentrations (~24 hrs after drug administration) were not significantly different with and without oral co-administration of ritonavir (Fig. 5, panel A). Plasma concentrations of ritonavir and docetaxel metabolites were below the limit of detection in all measured samples.

In tumor tissue, docetaxel concentrations on Day 9 were significantly higher (mean \sim 2.0-fold increased) when docetaxel was co-administered with ritonavir than after single docetaxel administration (Fig. 5b). Also on Day 16 there was a 2.0-fold higher mean tumor docetaxel concentration in the co-treated group, although this was not statistically significant. Ritonavir on Day 9 also showed markedly and significantly higher tumor concentrations in the co-treated group (Fig. 5d). However, for ritonavir one should be cautious with interpretation of tumor concentrations on Day 9 since this comparison might be biased by the substantial difference in tumor volume and histology in the ritonavir-treated group and docetaxel and ritonavir co-treated group (\sim 770 mm³ vs. \sim 170 mm³, respectively). Differences in abundance of cell types and structure within a tumor may affect the capacity to accumulate and retain certain drugs. This concern is less of a problem for docetaxel and docetaxel metabolite M2 concentrations, since the histology of docetaxel-treated tumors was comparable between groups treated with and without ritonavir. Tumor sizes on Day 9 were also more similar between the docetaxel-treated and co-treated groups (Fig. 2a).

The amount of the primary docetaxel metabolite M2 in tumor tissue was clearly much lower when docetaxel was co-administered with ritonavir on all days of measurement (Fig. 5, panel C). Docetaxel is metabolized via Cyp3a into metabolite M2 which is then further metabolized into other metabolites.^{46–48} M2 exhibits some cytotoxicity, however its cytotoxic effects are much lower than those of docetaxel. The other metabolites show no relevant cytotoxic activity.⁴⁹ A decrease in docetaxel tumor concentrations can be caused by both docetaxel metabolism and docetaxel efflux from the tumor tissue by drug transporters like P-gp. Given this, M2 tumor concentrations are a good parameter for assessment of altered docetaxel metabolism, since M2 formation is a direct functional result of docetaxel metabolism. Lower M2 tumor concentrations in docetaxel and ritonavir co-treated mice (Fig. 5c) suggest that docetaxel metabolism in the tumor was lower when docetaxel was co-administered with ritonavir than after single docetaxel administration. Decreased metabolism of docetaxel in the tumor could also explain the observed higher parent docetaxel concentrations in the tumor when docetaxel is co-administered with ritonavir (Fig. 5, panel B).

Docetaxel metabolism might be altered due to Cyp3a inhibition in the tumor by ritonavir or by altered Cyp3a expression in tumor tissue. Ritonavir could be readily detected and quantified in tumor tissue even 24 hrs after administration, indicating that Cyp3a inhibition in tumors by ritonavir is likely. As we did not observe a change in Cyp3a11, -3a13 or -3a16 expression in tumors, altered docetaxel metabolism seems not to be caused by a shift in Cyp3a expression. *Mdr1a* and *1b* expression in tumors was increased after repeated single docetaxel treatment (Figs. 4c and 4d), but co-administration of docetaxel and ritonavir resulted in similar changes in expression levels on Day 9 and 16. It cannot be excluded that the increased expression of *Mdr1a* and *Mdr1b* after docetaxel (co)treatment is related to selection of tumor

cells with comparatively higher *Mdr1a* and *Mdr1b* expression, which would reduce intracellular exposure of cells to docetaxel. This can result in a survival benefit for such cells and thus in a relatively high abundance of tumor cells with a high expression of *Mdr1*. Moreover, the increase in expression of *Mdr1a* and *1b* in docetaxel-treated tumors could also be related to the relative increase in tumor stroma in these tumors, as they are responding to the docetaxel therapy, if stroma has higher *Mdr1a* and *1b* expression than the initial tumor cells. Nonetheless, given the similar expression levels of *Mdr1* in docetaxel-treated mice with and without ritonavir co-treatment, it is not likely that *Mdr1a* and *1b* activity are a factor in the differentially increased antitumor activity as observed upon co-administration of docetaxel and ritonavir.

During the first week of treatment, tumor volumes were comparable in mice treated with docetaxel and in mice treated with both docetaxel and ritonavir. During the second week of treatment, we started to observe differences in tumor volume between these two groups (Figs. 2a and 2b). An increased antitumor activity of docetaxel and ritonavir co-treatment was clearly visible during the third and last week of treatment. This is in line with the observed differences in tumor concentrations of docetaxel and M2 over time (Fig. 5). On Day 2, tumor concentrations of M2 were low in docetaxel-treated mice and not detectable in docetaxel and ritonavir co-treated mice. While M2 was still undetectable on Day 9 and 16 in tumor tissue of co-treated mice, tumor concentrations of M2 increased over time after single docetaxel administration. In line with these observations, parent docetaxel concentrations were about twofold increased in the co-treated tumors. This suggests decreased docetaxel metabolism in tumors upon co-administration with ritonavir. Since detectable concentrations of ritonavir were still observed in tumor tissue 24 hr after administration, it is likely that ritonavir can extensively inhibit intratumoral Cyp3a. Given the absence of antitumor activity of single ritonavir treatment in our model, Cyp3a inhibition in the tumor by ritonavir may thus be primarily responsible for the observed increase in docetaxel activity when docetaxel is co-administered with ritonavir.

Conclusions

We found that antitumor activity of intravenously administered docetaxel in an immunocompetent, orthotopic mouse model for breast cancer is substantially increased by co-administration of orally administered ritonavir. Since we used mice lacking Cyp3a, this increase in activity is unlikely to be caused by altered systemic clearance of docetaxel. We could also exclude a differential shift in gene expression of Cyp3a and P-gp as a result of co-administration with ritonavir. Our data indicate that Cyp3a inhibition in tumor tissue by co-administered ritonavir decreased docetaxel metabolism in the tumor and this may have contributed to the observed increased antitumor activity of docetaxel.

Since CYP3A4 is expressed in multiple tumor types,^{9–13} these results reveal a potential additional advantage of co-administration of docetaxel and ritonavir, over that of its use to boost oral availability of docetaxel. We therefore believe

that it will also be worthwhile to test with various other tumor types whether co-administration of docetaxel and ritonavir will result in a higher antitumor activity.

References

- Grossi F, Kubota K, Cappuzzo F, et al. Future scenarios for the treatment of advanced non-small cell lung cancer: focus on taxane-containing regimens. *Oncologist* 2010;15:1102–12.
- Nishiyama M, Wada S. Docetaxel: its role in current and future treatments for advanced gastric cancer. *Gastric Cancer* 2009;12:132–41.
- Belfiglio M, Fanizza C, Tinari N, et al. Meta-analysis of phase III trials of docetaxel alone or in combination with chemotherapy in metastatic breast cancer. *J Cancer Res Clin Oncol* 2012;138:221–9.
- Cheatham P, Petrylak DP. Tubulin-targeted agents including docetaxel and cabazitaxel. *Cancer J* 2013;19:59–65.
- Koolen SL, Beijnen JH, Schellens JHM. Intravenous-to-oral switch in anticancer chemotherapy: a focus on docetaxel and paclitaxel. *Clin Pharmacol Ther* 2010;87:126–9.
- Schellens JHM, Malingre MM, Kruijtzter CM, et al. Modulation of oral bioavailability of anticancer drugs: from mouse to man. *Eur J Pharm Sci* 2000;12:103–10.
- Bardelmeijer HA, Ouweland M, Buckle T, et al. Low systemic exposure of oral docetaxel in mice resulting from extensive first-pass metabolism is boosted by ritonavir. *Cancer Res* 2002;62:6158–64.
- Oostendorp RL, Huitema A, Rosing H, et al. Coadministration of ritonavir strongly enhances the apparent oral bioavailability of docetaxel in patients with solid tumors. *Clin Cancer Res* 2009;15:4228–33.
- Kapucuoglu N, Coban T, Raunio H, et al. Expression of CYP3A4 in human breast tumour and non-tumour tissues. *Cancer Lett* 2003;202:17–23.
- Martinez C, Garcia-Martin E, Pizarro RM, et al. Expression of paclitaxel-inactivating CYP3A activity in human colorectal cancer: implications for drug therapy. *Br J Cancer* 2002;87:681–6.
- Murray GI, Shaw D, Weaver RJ, et al. Cytochrome P450 expression in oesophageal cancer. *Gut* 1994;35:599–603.
- Murray GI, Patimalla S, Stewart KN, et al. Profiling the expression of cytochrome P450 in breast cancer. *Histopathology* 2010;57:202–11.
- Zia H, Murray GI, Vyhldal CA, Leeder JS, Anwar AE, Bui MM, Ahmed AA. CYP3A isoforms in Ewing's sarcoma tumours: an immunohistochemical study with clinical correlation. *Int J Exp Pathol* 2015;96:81–6.
- Miyoshi Y, Ando A, Takamura Y, et al. Prediction of response to docetaxel by CYP3A4 mRNA expression in breast cancer tissues. *Int J Cancer* 2002;97:129–32.
- Zhong DS, Lu XH, Conklin BS, et al. HIV protease inhibitor ritonavir induces cytotoxicity of human endothelial cells. *Arterioscler Thromb Vasc Biol* 2002;22:1560–6.
- Pati S, Pelser CB, Dufraigne J, et al. Antitumorigenic effects of HIV protease inhibitor ritonavir: inhibition of Kaposi sarcoma. *Blood* 2002;99:3771–9.
- Sgadari C, Monini P, Barillari G, et al. Use of HIV protease inhibitors to block Kaposi's sarcoma and tumour growth. *Lancet Oncol* 2003;4:537–47.
- Gaedicke S, Firat-Geier E, Constantiniu O, et al. Antitumor effect of the human immunodeficiency virus protease inhibitor ritonavir: induction of tumor-cell apoptosis associated with perturbation of proteasomal proteolysis. *Cancer Res* 2002;62:6901–8.
- Maggiorella L, Wen B, Frascogna V, et al. Combined radiation sensitizing and anti-angiogenic effects of ionizing radiation and the protease inhibitor ritonavir in a head and neck carcinoma model. *Anticancer Res* 2005;25:4357–62.
- Srirangam A, Mitra R, Wang M, et al. Effects of HIV protease inhibitor ritonavir on Akt-regulated cell proliferation in breast cancer. *Clin Cancer Res* 2006;12:1883–96.
- Ahluwalia MS, Patton C, Stevens G, et al. Phase II trial of ritonavir/lopinavir in patients with progressive or recurrent high-grade gliomas. *J Neurooncol* 2011;102:317–21.
- Laurent N, de Boudard S, Guillamo JS, et al. Effects of the proteasome inhibitor ritonavir on glioma growth in vitro and in vivo. *Mol Cancer Ther* 2004;3:129–36.
- Ikezo T, Hisatake Y, Takeuchi T, et al. HIV-1 protease inhibitor, ritonavir: a potent inhibitor of CYP3A4, enhanced the anticancer effects of docetaxel in androgen-independent prostate cancer cells in vitro and in vivo. *Cancer Res* 2004;64:7426–31.
- Hendrikk JJ, Lagas JS, Rosing H, et al. P-glycoprotein and cytochrome P450 3A act together in restricting the oral bioavailability of paclitaxel. *Int J Cancer* 2013;132:2439–47.
- Li F, Wang L, Guo GL, et al. Metabolism-mediated drug interactions associated with ritonavir-boosted tipranavir in mice. *Drug Metab Dispos* 2010;38:871–8.
- van Waterschoot RA, Lagas JS, Wagenaar E, et al. Absence of both cytochrome P450 3A and P-glycoprotein dramatically increases docetaxel oral bioavailability and risk of intestinal toxicity. *Cancer Res* 2009;69:8996–9002.
- Bruno R, Hille D, Riva A, et al. Population pharmacokinetics/pharmacodynamics of docetaxel in phase II studies in patients with cancer. *J Clin Oncol* 1998;16:187–96.
- Sanli UA, Uslu R, Karabulut B, et al. Which dosing scheme is suitable for the taxanes? An in vitro model. *Arch Pharm Res* 2002;25:550–5.
- Harmsen S, Meijerman I, Beijnen JH, et al. Nuclear receptor mediated induction of cytochrome P450 3A4 by anticancer drugs: a key role for the pregnane X receptor. *Cancer Chemother Pharmacol* 2009;64:35–43.
- van Herwaarden AE, Wagenaar E, van der Kruijssen CM, et al. Knockout of cytochrome P450 3A yields new mouse models for understanding xenobiotic metabolism. *J Clin Invest* 2007;117:3583–92.
- Liu X, Holstege H, van der Gulden H, et al. Somatic loss of BRCA1 and p53 in mice induces mammary tumors with features of human BRCA1-mutated basal-like breast cancer. *Proc Natl Acad Sci USA* 2007;104:12111–6.
- Rottenberg S, Nygren AO, Pajic M, et al. Selective induction of chemotherapy resistance of mammary tumors in a conditional mouse model for hereditary breast cancer. *Proc Natl Acad Sci USA* 2007;104:12117–22.
- Euhus DM, Hudd C, LaRegina MC, et al. Tumor measurement in the nude mouse. *J Surg Oncol* 1986;31:229–34.
- Romijn JC, Verkoelen CF, Schroeder FH. Measurement of the survival of human tumor cells after implantation in athymic nude mice. *Int J Cancer* 1986;38:97–101.
- van Waterschoot RA, van Herwaarden AE, Lagas JS, et al. Midazolam metabolism in cytochrome P450 3A knockout mice can be attributed to up-regulated CYP2C enzymes. *Mol Pharmacol* 2008;73:1029–36.
- Livak KJ, Schmittgen TD. Analysis of relative gene expression data using real-time quantitative PCR and the 2(-Delta Delta C(T)) Method. *Methods* 2001;25:402–8.
- Yuan JS, Reed A, Chen F, et al. Statistical analysis of real-time PCR data. *BMC Bioinform* 2006;7:85.
- Hendrikk JJ, Hillebrand MJ, Thijssen B, et al. A sensitive combined assay for the quantification of paclitaxel, docetaxel and ritonavir in human plasma using liquid chromatography coupled with tandem mass spectrometry. *J Chromatogr B Analyt Technol Biomed Life Sci* 2011;879:2984–90.
- Hendrikk JJ, Dubbelman AC, Rosing H, et al. Quantification of docetaxel and its metabolites in human plasma by liquid chromatography/tandem mass spectrometry. *Rapid Commun Mass Spectrom* 2013;27:1925–34.
- Hendrikk JJ, Lagas JS, Wagenaar E, et al. Oral co-administration of elacridar and ritonavir enhances plasma levels of oral paclitaxel and docetaxel without affecting relative brain accumulation. *Br J Cancer* 2014;110:2669–76.
- Mauri D, Kamposioras K, Tsalis L, et al. Overall survival benefit for weekly vs. three-weekly taxanes regimens in advanced breast cancer: a meta-analysis. *Cancer Treat Rev* 2010;36:69–74.
- Kerbel RS. Human tumor xenografts as predictive preclinical models for anticancer drug activity in humans: better than commonly perceived-but they can be improved. *Cancer Biol Ther* 2003;2:S134–9.
- Suggitt M, Bibby MC. 50 years of preclinical anticancer drug screening: empirical to target-driven approaches. *Clin Cancer Res* 2005;11:971–981.
- Sharpless NE, Depinho RA. The mighty mouse: genetically engineered mouse models in cancer drug development. *Nat Rev Drug Discov* 2006;5:741–54.
- Rottenberg S, Vollebergh MA, de Hoon B, et al. Impact of intertumoral heterogeneity on predict-

Acknowledgement

We thank Wendy Sol for her help during tumor implantations and Anita van Esch for her help during RT-PCR analysis.

- ing chemotherapy response of BRCA1-deficient mammary tumors. *Cancer Res* 2012;72:2350–61.
46. Bardelmeijer HA, Roelofs AB, Hillebrand MJ, et al. Metabolism of docetaxel in mice. *Cancer Chemother Pharmacol* 2005;56:299–306.
47. Marre F, Sanderink GJ, de Sousa G, et al. Hepatic biotransformation of docetaxel (Taxotere) in vitro: involvement of the CYP3A subfamily in humans. *Cancer Res* 1996;56:1296–302.
48. Shou M, Martinet M, Korzekwa KR, et al. Role of human cytochrome P450 3A4 and 3A5 in the metabolism of taxotere and its derivatives: enzyme specificity, interindividual distribution and metabolic contribution in human liver. *Pharmacogenetics* 1998;8:391–401.
49. Sparreboom A, van Tellingen O, Scherrenburg EJ, et al. Isolation, purification and biological activity of major docetaxel metabolites from human feces. *Drug Metab Dispos* 1996;24:655–8.